

Towards Practical Privacy-Preserving Solution for Outsourced Neural Network Inference

Pinglan Liu, Wensheng Zhang

Department of Computer Science, Iowa State University, Ames, Iowa, USA 50011

E-mail: {pinglan,wzhang}@iastate.edu

Abstract—When neural network model and data are outsourced to cloud server for inference, it is desired to preserve the confidentiality of model and data as the involved parties (i.e., cloud server, model providing client and data providing client) may not trust mutually. Solutions were proposed based on multi-party computation, trusted execution environment (TEE) and leveled or fully homomorphic encryption (LHE/FHE), but their limitations hamper practical application. We propose a new framework based on synergistic integration of LHE and TEE, which enables collaboration among mutually-untrusted three parties, while minimizing the involvement of (relatively) resource-constrained TEE and allowing the full utilization of the untrusted but more resource-rich part of server. We also propose a generic and efficient LHE-based inference scheme as an important performance-determining component of the framework. We implemented/evaluated the proposed system on a moderate platform and show that, our proposed scheme is more applicable/scalable to various settings, and has better performance, compared to the state-of-the-art LHE-based solutions.

I. INTRODUCTION

As deep neural network based machine learning often demands large computational resource and data, outsourcing computation and data to cloud servers is popular. Outsourced data and neural network model can be exposed or stolen when they are at untrustable or vulnerable servers. Hence, we should protect their confidentiality; meanwhile, such protection should not prevent computations by authorized parties.

Extensive research has been conducted on protecting confidentiality of outsourced data and/or model. The adopted approaches roughly fall into the categories of multi-party computation (MPC), trusted execution environment (TEE), and leveled or fully homomorphic encryption (LHE/FHE). The MPC-based solutions [1]–[11] often also leverage partly homomorphic encryption. They have better computational efficiency, but at the expense of higher communication overhead and network latency, since multiple parties need to interact with each other while computation is being conducted. Some of them also have to assume no collusion between parties [12]–[15]. TEE-based solutions [16], [17] employ the hardware-based technologies such as Intel SGX to set up secure enclaves at the server to perform outsourced computation. Resource (e.g., memory) available at TEE is (relatively) constrained¹,

but the much more rich resources (including computationally-powerful GPUs) cannot be fully utilized. Thus, the scalability of such solutions can be limited.

LHE/FHE, which enables computation over encrypted data, is a promising tool for protecting data and model confidentiality while preserving its utility even in untrusted environment. Also, it does not require communication between multiple parties during computation and thus avoids the overhead and complexity due to communication; it can make use of the available computational (including GPUs) and memory resources. Its notoriously-high computation cost has long hampered it from being applied in practical systems, but theoretical and practical advancements [19]–[21] in the last decade are gradually changing the landscape. In particular, Smart and Vercauteren [20] proposed the packing technique, which indicates that, by packing a large number of values into the *slots* of a ciphertext, large-scale SIMD operations can be performed on these packed values at one time and hence the amortized cost can be significantly reduced. Applying LHE/FHE along with the packing technique, numerous research works [22]–[27] have been recently reported to protect data and model confidentiality for inference based on convolutional neural network (CNN). Among them, CryptoNets [22] and E2DM [23] are the most representative. However, CryptoNets assumes the availability of a large number of inputs to fill all the slots in each ciphertext. Though it has a high level of amortized efficiency, this may not be attainable in practice, where a client may not have a large set of inputs available at the same time. E2DM proposes a more sophisticated packing method that can efficiently utilize the slots when the number of simultaneously-available inputs is smaller. However, it only considers the CNN model with one convolutional layer and no generic method is provided for generic CNN models.

To address the limitations with the state of the art, we propose more practical framework and schemes to preserve the confidentiality of both neural network model and data outsourced to an untrusted server for inference. The main contributions of our work are as follows.

First, we propose a new framework that applies both LHE and TEE. With the framework, a cloud server first sets up a TEE, which initializes a LHE system. After attesting the TEE, a model providing client (i.e., model provider) uploads to the server its model parameters encrypted with the LHE public key provided by the TEE, and a data providing client (i.e., data provider) uploads to the server its input data encrypted

¹Taking Intel SGX as example, common CPUs have up to 128MB SGX memory; though some recent-generation Intel CPUs [18] support 8GB-512GB SGX memory, the size is still much smaller than that of their regular memory (up to 6TB); also, TEE has much higher paging overhead due to encryption.

with the same public key. The untrusted part of the server (i.e., REE - the resource-rich execution environment out of TEE), conducts the computation based on the encrypted model and data, and sends the inference result to the TEE, which decrypts the result, re-encrypts it with the data provider's secret key and sends it to the data provider. The proposed framework has the following advantages: it enables secure interactions among the three parties (model provider, data provider and cloud server), who may not trust mutually; it minimizes the involvement of the TEE, which is (relatively) constrained in resource, for only the most essential works of initializing the LHE system and decrypting/re-encrypting inference results; it allows the REE to be fully utilized in performing the outsourced computation.

Second, we propose a generic and efficient LHE-based inference scheme as an important performance-determining component of the proposed framework. With the scheme, a CNN model with arbitrary numbers of convolutional and fully-connected layers can be supported. Also, the model provider can specify a desired size of simultaneously-available inputs which can be much smaller than the total number of slots at a ciphertext. New packing methods and propagation algorithms are devised to efficiently pack the model parameters and the simultaneously-available inputs into ciphertexts and then efficiently process them, such that: ciphertexts are processed smoothly through all layers of a CNN model without decryption or re-encryption; the slots in ciphertexts are utilized as much as possible; the encryption level is minimized to reduce the size and processing complexity of ciphertexts.

Third, we implemented the proposed system and evaluated it extensively on a moderate platform. The evaluation results reported in this paper focuses on the following: Our system has good scalability with varying size of simultaneously-available inputs; the computational efficiency improves as the size increases, meanwhile it does not degrade significantly as the size decreases. Our system is applicable to various configurations of CNN model. Our system outperforms the state-of-the-art LHE-based schemes [22], [23], which is the most related to our work, in addition to that our system is applicable in more generic and practical settings.

In the rest of the paper, we present the background in Section II, our proposed framework in Section III, and our LHE-based inference scheme in Section IV. Section V reports our evaluation results, and Section VI briefly surveys the related works. Finally, Section VII concludes the paper.

II. PRELIMINARIES

A. System Model and Problem Description

We consider a system composed of a cloud server and multiple clients. The server consists of trusted execution environments (TEEs) each could be an Intel SGX [28] enclave that has been successfully attested, and a untrusted but resource-rich execution environment (called REE, i.e., execution environment outside of any SGX enclave). Note that, side-channel attacks to TEE and the corresponding mitigation techniques have been extensively studied and are out of the scope of this paper. Deploying any mitigation technique is orthogonal to

and thus can be integrated with our proposed design. Also, as our design tries to minimize the involvement of TEE (i.e., TEE is only used for key generation/distribution and the decryption/re-encryption of inference results), we anticipate that deploying mitigation techniques should not affect the system performance much.

There are two types of clients, a model provider and multiple data providers. The model provider owns a neural network model (e.g., a CNN model for image classification) that it has already trained. Each data provider has data (e.g., images) that can be processed with the neural network model. The clients want the cloud server to use the model to make inference based on the data. Meanwhile, data and model privacy should remain confidential. Specifically, the data should not be revealed to anyone other than its providing client and the model parameters should not be revealed to anyone other than its providing client. However, we allow the hyper-parameters of the model (including the number of layers and the number of nodes on each layer) to be revealed.

B. CNN Model

For a CNN model outsourced by its provider, we assume that it consists of a sequence of c convolutional layers (called CLs) followed by f fully-connected layers (called FLs).

For each convolutional layer $l \in \{0, \dots, c-1\}$, we assume that it has α_l channels, one input matrix for a channel is of $\beta_l \times \beta_l$ elements (thus β_l is *side* of an input matrix of the layer), it has ϵ_l filters for each channel, the side of a filter is denoted as γ_l and the stride is denoted as δ_l . For each fully-connected layer $l \in \{0, \dots, f-1\}$, the numbers of input and output neurons are denoted as u_l and o_l , respectively. Thus, its weight matrix, denoted as $M^{(l)}$, has dimensions $u_l \times o_l$.

For simplicity, we assume the square function is used as the activation function for each layer, as in [22], [23]. Note that, there have also been extensive studies on the evaluation of various activation functions over encrypted data [29]–[31]. Such schemes can be integrated with our proposed scheme, but do not elaborate on this as it is out of the scope of this paper.

C. Homomorphic Encryption Primitives

We use an asymmetric leveled homomorphic encryption (LHE) scheme, which enables the computation on encrypted data (i.e., ciphertexts) as long as the computations do not exceed a certain predefined *level*. We also assume that the scheme adopts the ciphertext packing technique, with which multiple values can be encoded and encrypted into a single ciphertext and operations can be performed in a SIMD manner. Formally, the LHE scheme has the following primitives:

- $(sk, pk, evk) \leftarrow KeyGen(1^\lambda, \mathcal{L})$: given security parameter λ and the highest level of encryption \mathcal{L} , it outputs a secret key sk , a public key pk , an evaluation key evk and the slot number S for each ciphertext. Here, S is also the number of scalar values that can be encoded and encrypted to a ciphertext.

- $ct \leftarrow Enc_{pk}(\vec{pt})$: given public key pk and a plaintext vector $\vec{pt} = (pt_0, \dots, pt_{S-1})$, it outputs ciphertext ct .
- $\vec{pt} \leftarrow Dec_{sk}(ct)$: given secret key sk and a ciphertext ct , it outputs plaintext vector \vec{pt} whose values are encoded and encrypted to ct .
- $ct' \leftarrow ct_1 \oplus ct_2$: given ciphertexts ct_1 and ct_2 , it outputs ciphertext ct' s.t. $Dec_{sk}(ct') = Dec_{sk}(ct_1) + Dec_{sk}(ct_2)$. Note that, the $+$ operator stands for element-wise addition between two vectors; that is, if $Dec_{sk}(ct_1) = \vec{pt}_1 = (pt_{1,0}, \dots, pt_{1,S-1})$ and $Dec_{sk}(ct_2) = \vec{pt}_2 = (pt_{2,0}, \dots, pt_{2,S-1})$, then $Dec_{sk}(ct_1) + Dec_{sk}(ct_2) = (pt_{1,0} + pt_{2,0}, \dots, pt_{1,S-1} + pt_{2,S-1})$.
- $ct' \leftarrow ct_1 \otimes ct_2$: given ciphertexts ct_1 and ct_2 , it outputs ciphertext ct' s.t. $Dec_{sk}(ct') = Dec_{sk}(ct_1) \times Dec_{sk}(ct_2)$. Note that, the \times operator stands for element-wise multiplication between two vectors; that is, if $Dec_{sk}(ct_1) = \vec{pt}_1 = (pt_{1,0}, \dots, pt_{1,S-1})$ and $Dec_{sk}(ct_2) = \vec{pt}_2 = (pt_{2,0}, \dots, pt_{2,S-1})$, then $Dec_{sk}(ct_1) \times Dec_{sk}(ct_2) = (pt_{1,0} \times pt_{2,0}, \dots, pt_{1,S-1} \times pt_{2,S-1})$.
- $ct' \leftarrow CMult(ct, \vec{pt})$: given ciphertext ct and plaintext \vec{pt} , it outputs ciphertext ct' s.t. $Dec_{sk}(ct') = \vec{pt} \times Dec_{sk}(ct)$.
- $ct' \leftarrow Rot(ct, m)$: given ciphertext ct that encrypts $\vec{pt} = (pt_0, \dots, pt_{S-1})$ and integer $m < S$, it outputs ct' which is ciphertext for $(pt_m, \dots, pt_{S-1}, pt_0, \dots, pt_{m-1})$.

Note that, the operations involving ciphertext, i.e., \otimes , $CMult$ and Rot , use some keys which are skipped here for brevity. In our design and implementation, we adopt CKKS [21], which provides all the above primitives that we need.

III. PROPOSED FRAMEWORK

Figure 1: Framework of Proposed Solution.

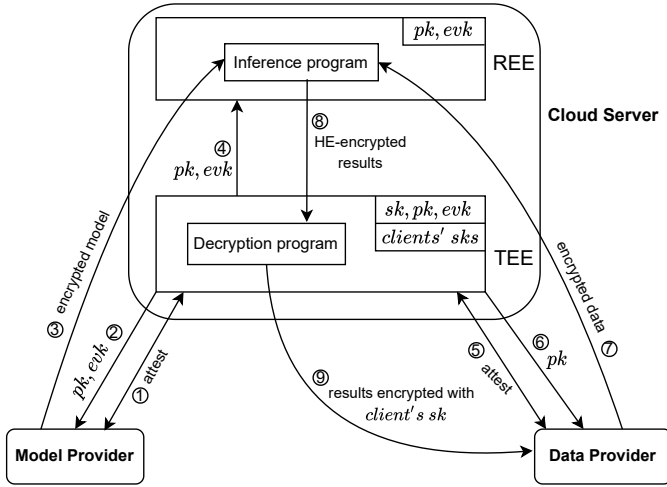


Figure 1 illustrates the framework of our proposed solution, which is explained as follows. The framework involves four parties: the TEE of the cloud server, the REE of the cloud server, the model provider, and the data provider. The interactions among these parties are as follows: ① The model provider attests the TEE. Once the attestation succeeds, it

shares its secret key and the hyper-parameters of its outsourced CNN model with the TEE. ② Based on the CNN model's architecture, the TEE calls algorithm *GenKey* to randomly generate the keys for asymmetric leveled homomorphic encryption and securely sends the public key pk to the model provider. ③ The model provider encrypts its model parameters and then uploads the encrypted parameters to the REE. ④ The TEE sends pk and the evaluation key evk to the REE. ⑤ The data provider attests the TEE. Once the attestation succeeds, it shares its secret key with the TEE. ⑥ TEE securely sends pk to the data Provider. ⑦ The data provider encodes and encrypts its data and uploads the encrypted data to the REE. ⑧ The REE conducts the inference based on encrypted model and encrypted data, and sends the inference result to TEE for decryption. ⑨ The TEE decrypts the result, and returns to the data provider the result after it has been further encrypted with the data provider's secret key. ⑩ The data provider decrypts the result with its secret key.

Next, we elaborate on steps ②, ③, ⑦ and ⑧, which form the LHE-based efficient inference scheme, a performance-determining component of the proposed framework.

IV. LHE-BASED INFERENCE SCHEME

To support confidentiality-preserving inference with a CNN model of c convolutional layers and f fully connected layers, the TEE first determines the highest encryption level \mathcal{L} based on the topology of the model. Specifically, if each layer consumes two encryption levels (as for the CNN model specified in Sec. II-B), it can set $\mathcal{L} = 2(c + f)$. Next, the TEE initializes an LHE system by calling *KeyGen*($2^\lambda, \mathcal{L}$) to obtain the keys; note that, we set security parameter λ to 128 in our implementation. The public and evaluation keys are then distributed to the Server's REE and the clients, while the private key is kept only by the TEE.

A. Encoding and Encrypting Input Data and Filters

In Steps ③ and ⑦ of the proposed framework, the model provider should encode and encrypt its model parameters, and the data provider should encode and encrypt its input data, before they upload them to the server.

1) *The Rationale*: To understand our proposed design, let us first briefly review the packing method in E2DM [23]. We start with the simplest scenario where there is only one channel and one input matrix I with β_0^2 values. Following the notations introduced in Section II-B, let the only convolutional layer have kernel side γ_0 and stride δ_0 . The method packs the β_0^2 values into γ_0^2 ciphertexts. Denoting the ciphertexts as $\hat{C}_{i,j}$ for every $(i, j) \in \{0, \dots, \gamma_0 - 1\}^2$, each $\hat{C}_{i,j}$ encrypts the vector that packs all the values $I_{u,v}$ where $u - i$ and $v - j$ are multiples of stride δ_0 . Accordingly, each element $F_{i,j}$ of each filter matrix F is replicated to fill a vector and then encoded/encrypted to ciphertext $\hat{F}_{i,j}$; propagating through this layer results in a ciphertext $\sum_{0 \leq i,j \leq \gamma_0 - 1} \hat{C}_{i,j} \otimes \hat{F}_{i,j}$. Note that, when there are multiple input matrices for a channel, the above method can be straightly extended to have each ciphertext $\hat{C}_{i,j}$

pack and encrypt all the values $I_{u,v}$ from every input matrices I where $u - i$ and $v - j$ are multiples of δ_0 .

To facilitate propagation through all the c convolutional layers with packing/encryption only needed at the very beginning, intuitively, we aim to encode/encrypt each input matrix as if there were only one *combined layer* that virtually includes all the c layers in order. We denote the parameters of the combined layer as:

- $\tilde{\delta}_0$ for *combined stride*, and
- $\tilde{\gamma}_0$ for *combined kernel side* (i.e., $\tilde{\gamma}_0^2$ is the number of encrypted inputs for each channel).

For convenience, we extend this notation and treat the combination of sequential layers from l (where $0 \leq l < c$) to $c-1$ as *combined layer from l* ; thus, $\tilde{\delta}_l$ denotes *combined stride* and $\tilde{\gamma}_l$ denotes *combined kernel side* for such a combined layer.

In our proposed design, we aim to pack and encrypt data in a way that should meet the following requirements at each convolutional layer l : First, $\tilde{\gamma}_l \geq \gamma_l$; this is necessary as the input values should be multiplied with γ_l^2 elements of each filter respectively. Second, due to the rule of forward propagation through a convolutional layer, following relation should hold for the side $\tilde{\gamma}_l$ of each encrypted input matrix and the side of each output matrix (which is also the side $\tilde{\gamma}_{l+1}$ of each encrypted input matrix for layer $l+1$ when $l < c-1$):

$$\tilde{\gamma}_{l+1} = 1 + \lfloor \frac{\tilde{\gamma}_l - \gamma_l}{\delta_l} \rfloor. \quad (1)$$

Third, also due to the rule of the forward propagation, following relation should hold between $\tilde{\delta}_l$ and $\tilde{\delta}_{l+1}$:

$$\tilde{\delta}_l = \delta_l \cdot \tilde{\delta}_{l+1}. \quad (2)$$

Particularly for the last convolutional layer, $\tilde{\delta}_{c-1} = \delta_{c-1}$. Setting $\tilde{\gamma}_{c-1} = \gamma_{c-1}$ and guided by the above requirements, we can derive the following general settings of the parameters for each layer l :

$$\tilde{\gamma}_l = 1 + \sum_{i=l}^{c-1} (\gamma_i - 1) \prod_{j=0}^{i-1} \delta_j, \quad (3)$$

and

$$\tilde{\delta}_l = \prod_{i=l}^{c-1} \delta_i. \quad (4)$$

Based on the above parameter settings, we elaborate our proposed method for encoding and encryption in the following.

2) *Encoding and Encrypting Input Data*: For each channel i , all of its n input matrices are encoded as follows. Let these matrices be denoted as $I_i^{(j)}$ for every $j \in \{0, \dots, n-1\}$, and each value of $I_i^{(j)}$ be denoted as $I_{i,x,y}^{(j)}$ for $x, y \in \{0, \dots, \beta_0 - 1\}$. All the values are encoded/encrypted into $\tilde{\gamma}_0^2$ ciphertexts, each indexed by (i, u, v) for $(u, v) \in \{0, \dots, \tilde{\gamma}_0 - 1\}^2$. Each ciphertext $\hat{C}_{i,u,v}^{(0)}$ encodes/encrypts the following vector:

$$\begin{pmatrix} \vec{I}_{i,u,v} & \vec{I}_{i,u,v+\tilde{\delta}_0} & \cdots & \vec{I}_{i,u,v+(\tilde{\beta}_0-1)\tilde{\delta}_0} \\ \vec{I}_{i,u+\tilde{\delta}_0,v} & \vec{I}_{i,u+\tilde{\delta}_0,v+\tilde{\delta}_0} & \cdots & \vec{I}_{i,u+\tilde{\delta}_0,v+(\tilde{\beta}_0-1)\tilde{\delta}_0} \\ \vdots & \vdots & \ddots & \vdots \\ \vec{I}_{i,u+(\tilde{\beta}_0-1)\tilde{\delta}_0,v} & \vec{I}_{i,u+(\tilde{\beta}_0-1)\tilde{\delta}_0,v+\tilde{\delta}_0} & \cdots & \vec{I}_{i,u+(\tilde{\beta}_0-1)\tilde{\delta}_0,v+(\tilde{\beta}_0-1)\tilde{\delta}_0} \end{pmatrix}, \quad (5)$$

where for each $(x, y) \in \{0, \dots, \tilde{\gamma}_0 - 1\}^2$,

$$\vec{I}_{i,x,y} = (I_{i,x,y}^{(0)}, \dots, I_{i,x,y}^{(n-1)}). \quad (6)$$

3) *Encoding and Encrypting Filters*: Due to the above method for encoding/encrypting input data, all the values encoded/encrypted in one same ciphertext needs to be multiplied with one same element of a filter at a time. Hence, each element $F_{i,j}$ of a filter F should be duplicated for $n \cdot \tilde{\beta}_0^2$ times and then encoded/encrypted into a ciphertext denoted as $\hat{F}_{i,j}$.

B. Propagation through Convolutional Layer l

With the above method for encoding and encryption, each propagation layer l has $\tilde{\gamma}_l^2$ input ciphertexts for each channel; they can be treated as elements of an encrypted input matrix of dimensions $\tilde{\gamma}_l \times \tilde{\gamma}_l$. We denote these input ciphertexts as $\hat{C}_{i,u,v}^{(l)}$ for every channel $i \in \{0, \dots, \alpha_l - 1\}$ and every pair $(u, v) \in \{0, \dots, \tilde{\gamma}_l - 1\}^2$. Convolutional operations are then performed between these input ciphertexts and the encrypted elements of the filters. The encrypted elements of the filters are denoted as $\hat{F}_{i,x,y}^{(l,k)}$ for every channel i , every filter with index $k \in \{0, \dots, \epsilon_l - 1\}$ of the channel, and every element index $(x, y) \in \{0, \dots, \gamma_l - 1\}^2$ of a filter matrix. Then, the activation function, which is a square function in this paper, is applied at each of the resulting neurons. Finally, propagating through the layer results in the following outputs: $\hat{C}_{k,u,v}^{(l+1)}$ for every output channel $k \in \{0, \dots, \epsilon_l - 1\}$ and every pair $(u, v) \in \{0, \dots, \tilde{\gamma}_{l+1} - 1\}^2$. Note that, the outputs become the inputs of the next layer; when $l = c = 1$, each output channel has only one output ciphertext, i.e., $\tilde{\gamma}_c = 1$. The procedure is formally presented in Algorithm 1.

Algorithm 1: Propagation through Conv. Layer l

```

1 for  $k \in \{0, \dots, \epsilon_l - 1\}$  do
2   for  $(u, v) \in \{0, \dots, \tilde{\gamma}_{l+1} - 1\}^2$  do
3      $\hat{C}_{k,u,v}^{(l+1)} \leftarrow 0$ ;  $\triangleright$  initialize each output;
4      $(u', v') \leftarrow (\delta_l \cdot u, \delta_l \cdot v)$ ;
5     for  $(x, y) \in \{0, \dots, \gamma_l - 1\}^2$  do
6       for  $i \in \{0, \dots, \alpha_l - 1\}$  do
7          $\hat{C}_{k,u,v}^{(l+1)} \oplus = \hat{C}_{i,u'+x,v'+y}^{(l)} \otimes \hat{F}_{i,x,y}^{(l,k)}$ ;
8       end
9     end
10     $\hat{C}_{k,u,v}^{(l+1)} \leftarrow \hat{C}_{k,u,v}^{(l+1)} \otimes \hat{C}_{k,u,v}^{(l+1)}$ ;  $\triangleright$  activation
11  end
12 end
```

C. Propagation through Fully-connected Layer l

Recall that the input to layer l is the intermediate results of processing n original inputs, and the processing for these n inputs are in parallel independently. Due to our method for encoding (as in Section IV-A), the input values that are of the same offset but from n different original inputs are encoded consecutively (as in Eq. (6)), we call such sequence of n values as a *parallel input set (pi-set)*. We use ι_l to denote the number of pi-sets encoded/encrypted into the input of layer l ; thus, the input of layer l encodes/encrypts totally $\iota_l \cdot n$ values. We further use ι'_l to denote the number of ciphertexts in the input to layer l , and denote the ciphertexts as $\hat{C}_0^{(l)}, \dots, \hat{C}_{\iota'_l-1}^{(l)}$. Our design evenly distributes the ι_l pi-sets to the ι'_l ciphertexts; thus, each ciphertext encodes/encrypts $\iota_l'' = \frac{\iota_l}{\iota'_l}$ pi-sets. We also assume ι_l'' is an integer for the convenience of presentation.

The input to layer l has two types. Type I (ciphertext input without replication): each ciphertext encodes/encrypts multiple pi-sets in the format similar to Eq. (5) and (6), in which the pi-sets are not replicated. Type II (ciphertext input with replication): each ciphertext contains one pi-set which is replicated for multiple times. Next, we present the algorithms for propagating through layer l with each type of input.

1) *Propagation with Type I Input:* In this case, each input ciphertext $\hat{C}_j^{(l)}$ for $j \in \{0, \dots, \iota'_l - 1\}$ encodes and encrypts ι_l'' pi-sets. As presented in Section II-B, the weight matrix for the layer is $M^{(l)}$ with dimensions $\iota_l \times o_l$; let us denote the elements of $M^{(l)}$ as $M_{u,v}^{(l)}$ where $u \in \{0, \dots, o_l - 1\}$ and $v \in \{0, \dots, \iota_l - 1\}$. To facilitate efficient forward propagation through this layer, the elements of $M^{(l)}$ are encoded and encrypted to $o_l \cdot \iota'_l$ ciphertexts, denoted as $\hat{M}_{i,j}^{(l)}$ for every $i \in \{0, \dots, o_l - 1\}$ and every $j \in \{0, \dots, \iota'_l - 1\}$. Here, each $\hat{M}_{i,j}^{(l)}$ encrypts the following vector

$$(\vec{M}_{i,j \cdot \iota_l'', \dots, (j+1) \cdot \iota_l'' - 1}^{(l)}), \quad (7)$$

where for each $w \in \{j \cdot \iota_l'', \dots, (j+1) \cdot \iota_l'' - 1\}$, $\vec{M}_{i,w}^{(l)}$ stands for a sequence of n duplicated values of $M_{i,w}^{(l)}$; i.e.,

$$\vec{M}_{i,w}^{(l)} = (M_{i,w}^{(l)}, \dots, M_{i,w}^{(l)}). \quad (8)$$

Algorithm 2 formally presents the forward propagation. This results in o_l ciphertexts, each encoding/encrypting $\frac{\iota_l}{n}$ replicas of a set of n output values. Note that, if the output is used as the input of the next layer, it becomes a type II input.

2) *Propagation with Type II Input:* In this case, the input has $\iota'_l = \iota_l$ ciphertexts each encrypting $\frac{\iota_l}{n}$ replicas of only one input set (i.e., n input values from n original inputs). To facilitate the propagation, the elements of weight matrix $M^{(l)}$ are encrypted to $\iota_l \cdot \lceil \frac{o_l \cdot n}{S} \rceil$ ciphertexts, denoted as $\hat{M}_{i,j}^{(l)}$ for $i \in \{0, \dots, \iota_l - 1\}$ and $j \in \{0, \dots, \lceil \frac{o_l \cdot n}{S} \rceil - 1\}$, where each $\hat{M}_{i,j}^{(l)}$ encodes and encrypts the following vector

$$(\vec{M}_{j \cdot \frac{\iota_l}{n}, i}^{(l)}, \dots, \vec{M}_{\min\{(j+1) \cdot \frac{\iota_l}{n}, o_l\} - 1, i}^{(l)}), \quad (9)$$

where for each $w \in \{j \cdot \frac{\iota_l}{n}, \dots, \min\{(j+1) \cdot \frac{\iota_l}{n}, o_l\} - 1\}$, $\vec{M}_{w,i}^{(l)}$ stands for a sequence of n duplicated values of $M_{w,i}^{(l)}$.

Algorithm 2: Propagation through Fully-connected Layer l (with Type I Input)

```

1 for  $i \in \{0, \dots, o_l - 1\}$  do
2    $\hat{C}_i^{(l+1)} \leftarrow 0$ ;  $\triangleright$  initialize each output ciphertext;
3   for  $j \in \{0, \dots, \iota'_l - 1\}$  do
4      $\hat{C}_i^{(l+1)} \oplus = \hat{C}_j^{(l)} \otimes \hat{M}_{i,j}^{(l)}$ ;
5   end
6   for  $j \in \{1, \dots, \log(\frac{\iota_l}{n})\}$  do
7      $\hat{C}_i^{(l+1)} \oplus = \text{Rot}(\hat{C}_i^{(l+1)}, j \cdot n)$ ;
8   end
9    $\hat{C}_i^{(l+1)} \leftarrow \hat{C}_i^{(l+1)} \otimes \hat{C}_i^{(l+1)}$ ;  $\triangleright$  activation
10 end

```

Algorithm 3 formally presents how the forward propagation is conducted through a type-II fully-connected layer l . This results in $\lceil \frac{o_l \cdot n}{S} \rceil$ ciphertexts each encoding/encrypting $\frac{\iota_l}{n}$ pi-sets. Note that, if the output is used as the input for the next layer, it becomes a Type I input.

Algorithm 3: Propagation through Fully-connected Layer l (with Type II Input)

```

1 for  $i \in \{0, \dots, \lceil \frac{o_l \cdot n}{S} \rceil - 1\}$  do
2    $\hat{C}_i^{(l+1)} \leftarrow 0$ ;  $\triangleright$  each output element  $i$ ;
3   for  $j \in \{0, \dots, \iota_l - 1\}$  do
4      $\hat{C}_i^{(l+1)} \oplus = \hat{C}_j^{(l)} \otimes \hat{M}_{i,j}^{(l)}$ 
5   end
6    $\hat{C}_i^{(l+1)} \leftarrow \hat{C}_i^{(l+1)} \otimes \hat{C}_i^{(l+1)}$ ;  $\triangleright$  activation
7 end

```

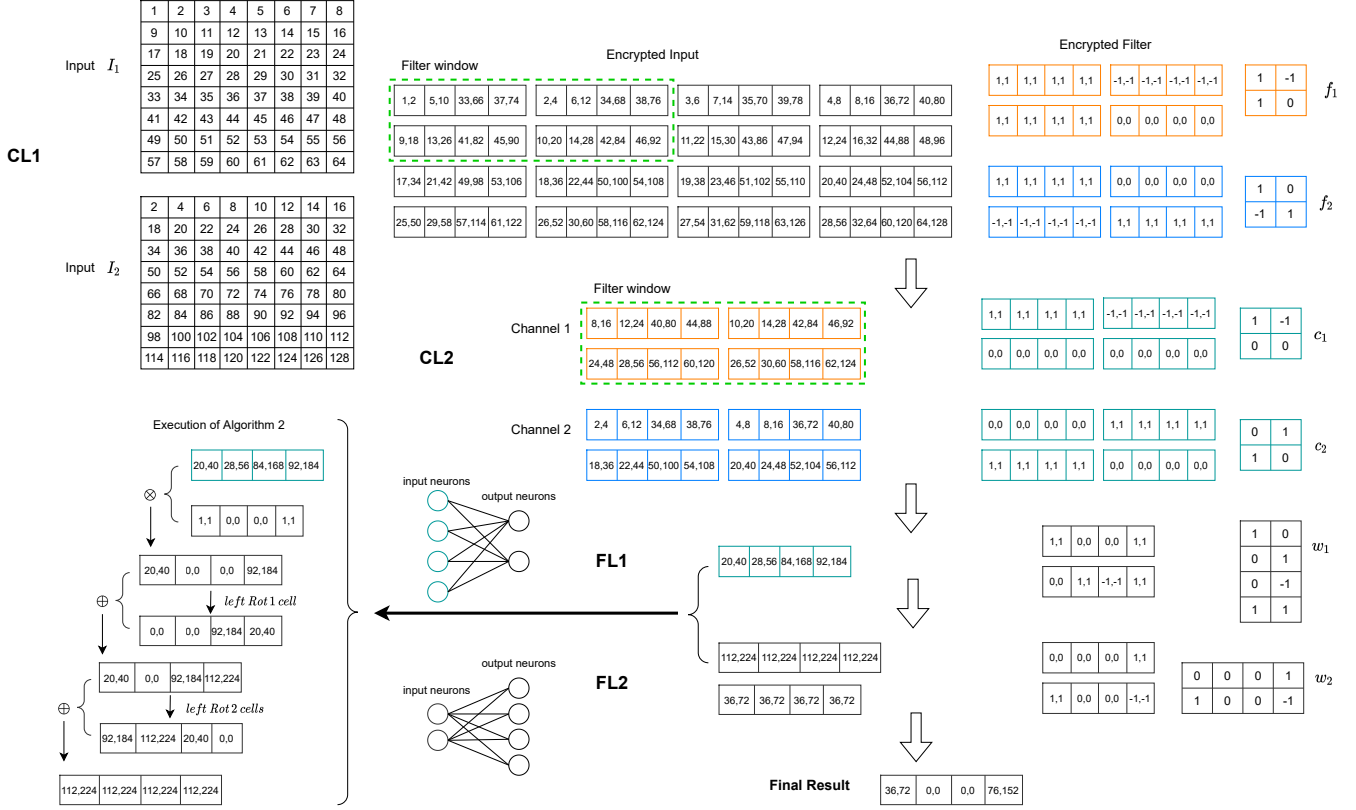
D. An Example

Figure 2 illustrates a simple example, where our proposed scheme is applied to a CNN model of 2 CLs and 2 FLs and activation function is not considered. Two 8×8 input matrices, labelled as I_1 and I_2 , are processed in parallel. Thus, 16 ciphertexts are constructed to encode/encrypt the values of the input matrices. Each ciphertext encodes/encrypts 8 input values, represented as 4 cells. Each cell contains 2 values from the 2 input matrices respectively; recall that such a cell is called pi-set in the description of our scheme.

CL1 has two 2×2 filter matrices, labelled as f_1 and f_2 , each has one channel. CL2 also has two 2×2 filters, labelled as c_1 and c_2 , each belonging to a separated channel. Each filter is encrypted to 4 ciphertexts, and each ciphertext contains 8 replicated elements to match the ciphertexts for input values. The output from the two CLs is one single ciphertext, which is a Type I input to layer FL1.

FL1 has 4 input and 2 output neurons as inferred from its 4×2 weight matrix. The elements of the matrix is encrypted to 2 ciphertexts corresponding to the 2 output neurons respectively. Now, the outputs should be computed as the dot-products of the vector encoded/encrypted in the input

Figure 2: An Example.



ciphertext and each of the vectors encoded/encrypted in the weight-matrix's ciphertexts. This is accomplished according to Algorithm 2, and the call-out on the left-hand side illustrates the steps for computing the first of the outputs:

First, the input ciphertext that encrypts $(20, 40, 28, 56, 84, 168, 92, 184)$ HE-multiplies with the first ciphertext of the weight matrix, which encrypts $((1, 1, 0, 0, 0, 0, 1, 1))$; this results in the ciphertext that encrypts $(20, 40, 0, 0, 0, 0, 92, 184)$.

Second, the ciphertext for $(20, 40, 0, 0, 0, 0, 92, 184)$ HE-adds a copy of itself which but also rotates (to left) for one cell, and this results in a ciphertext for $(20, 40, 0, 0, 92, 184, 112, 224)$.

Third, the ciphertext for HE-adds a copy of itself which also rotates (to left) for 2 cells, and this results in a ciphertext for $(112, 224, 112, 224, 112, 224, 112, 224)$.

The result of the above steps becomes a type II input for the next layer, FL2. For FL2, the weights connected to the same input neuron are packed into one ciphertext; hence, there are 2 ciphertexts for the weights. Each of the 2 ciphertexts multiplies with the corresponding input ciphertext, and resulting 2 product-ciphertexts are added up to get the final result, which encrypts $(36, 72, 0, 0, 0, 0, 76, 152)$.

V. OPTIMIZATIONS ON PACKING

With the above scheme, each initial input ciphertext encodes/encrypts $n \cdot \beta_0^2$ input values. If $n \cdot \beta_0^2$ is much less

than \mathcal{S} (i.e., the number of available slots in a ciphertext), the slots will not be effectively utilized and the computation/communication efficiency will be negatively affected. To address this limitation, we propose cross-channel and cross-filter packing in this section. Specifically, letting r be the largest power of two which is no greater than $\frac{\mathcal{S}}{n \cdot \beta_0^2}$, the inputs from r channels can be encoded together such that more input values can be processed in parallel, or each ciphertext can encode/encrypt r replicas of the original $n \cdot \beta_0^2$ values such that the same input can be processed with multiple filters in parallel. Such changes, however, also demand according changes to the procedure of propagation through each convolutional layer. In this section, we elaborate on these optimizations.

A. Cross-Channel Packing

With cross-channel packing, input values from r different channels can be encoded/encrypted into one ciphertext; accordingly, the elements of the filters associated with these channels should be encoded together accordingly. Such a design reduces the number of input ciphertexts at convolutional layer l to $\lceil \frac{\alpha_l}{r} \rceil$ and reduces the number of ciphertexts that encode/encrypt filters to $\epsilon_l \lceil \frac{\alpha_l}{r} \rceil \beta_l^2$.

More specifically, all the α_l channels at layer l are grouped into $\lceil \frac{\alpha_l}{r} \rceil$ groups, where each channel group i' includes channels $\{i' \cdot r, \dots, \min\{(i' + 1) \cdot r, \alpha_0\} - 1\}$. All the plaintext input values to this layer are now encoded/encrypted into ciphertexts $\tilde{C}_{i',u,v}^{(l)}$ for every $i' \in \{0, \dots, \lceil \frac{\alpha_l}{r} \rceil - 1\}$ and every

$(u, v) \in \{0, \dots, \tilde{\gamma}_l - 1\}^2$. Here, each $\tilde{C}_{i',u,v}^{(l)}$ encodes/encrypts the concatenation of r vectors formatted as as Eq. (5) and (6) for every $i \in \{i' \cdot r, \dots, \min\{(i' + 1) \cdot r, \alpha_l\} - 1\}$. Accordingly, for every i' , every $k \in \{0, \epsilon_l - 1\}$ and every $(x, y) \in \{0, \dots, \beta_l - 1\}^2$, a ciphertext $\hat{F}_{i',x,y}^{(l,k)}$ is constructed to encode/encrypt the elements with index (x, y) , which is replicated for n copies, of the k -th filters in every channels of channel group i' .

Based on the above encryption strategy, the procedure of propagation through this layer is formalized in Algorithm 4. As we can see, most part of this algorithm is similar to Algorithm 1, but it reduces the iteration number from α_l to $\lceil \frac{\alpha_l}{r} \rceil$ in the innermost layer of loop (lines 6-9). The algorithm further employs rotation to sum up subsets of the elements encoded/encrypted in each ciphertext, which is similar to Algorithm 2. Each ciphertext output by this algorithm contains r replicas of data set encoded/encrypted in the cross-filter pattern. If the output is used as the input of next convolutional layer, they can be processed as described next.

Algorithm 4: Propagation Through Convolutional Layer l with Cross-Channel Packing

```

1 for  $k \in \{0, \dots, \epsilon_l - 1\}$  do
2   for  $(u, v) \in \{0, \dots, \tilde{\gamma}_{l+1} - 1\}^2$  do
3      $\hat{C}_{k,u,v}^{(l+1)} \leftarrow 0$ ;  $\triangleright$  each element of output matrix;
4      $(u', v') \leftarrow (\delta_l \cdot u, \delta_l \cdot v)$ ;
5     for  $(x, y) \in \{0, \dots, \gamma_l - 1\}^2$  do
6       for  $i' \in \{0, \dots, \lceil \frac{\alpha_l}{r} \rceil - 1\}$  do
7          $\triangleright$  iterating each channel group;
8          $\hat{C}_{k,u,v}^{(l+1)} \oplus = \hat{C}_{i',u'+x,v'+y}^{(l)} \otimes \hat{F}_{i',x,y}^{(l,k)}$ ;
9       end
10    end
11    for  $j \in \{1, \dots, \log(r)\}$  do
12       $\tilde{C}_{k,u,v}^{(l+1)} += \text{Rot}(\tilde{C}_{k,u,v}^{(l+1)}, j \cdot n \cdot \tilde{\beta}_0^2)$ ;
13    end
14     $\hat{C}_{k,u,v}^{(l+1)} \leftarrow \hat{C}_{k,u,v}^{(l+1)} \otimes \tilde{C}_{k,u,v}^{(l+1)}$ ;  $\triangleright$  activation
15  end
16 end

```

B. Cross-Filter Packing

With cross-filter packing, distinct input values are packed as pi-sets and then all these distinct values as whole is replicated for r times. Specifically for a layer l with cross-filter packing input, the input includes $\alpha_l \cdot \tilde{\gamma}_l^2$ ciphertexts. Each ciphertext $\hat{C}_{i,u,v}^{(l)}$ for channel $i \in \{0, \dots, \alpha_l - 1\}$ and $(u, v) \in \{0, \dots, \tilde{\gamma}_l - 1\}^2$ encodes/encrypts r replicas of the β_l pi-sets that are formatted similarly to Eq. (5) and (6).

The existence of replication in the ciphertexts provides an opportunity for each ciphertext to be multiplied with a ciphertext encoding/encrypting elements from multiple filters at a time; this way, increased level of parallel processing can be attained. Specifically, for each channel i , all the ϵ_l filter matrices are grouped into $\lceil \frac{\epsilon_l}{r} \rceil$ groups such that each

group $k' \in \{0, \dots, \lceil \frac{\epsilon_l}{r} \rceil - 1\}$ contains filters $\tilde{F}^{(l,k')}$ for every $k \in \{k' \cdot r, \dots, \min\{(k' + 1) \cdot r, \epsilon_l\} - 1\}$. Then, for every such filter group k' and every pair $(x, y) \in \{0, \dots, \beta_l - 1\}^2$, a ciphertext $\hat{F}_{i,x,y}^{(l,k')}$ is constructed to encode/encrypt every element with index (x, y) , which is replicated for n copies, of every filters in group k' of channel i .

Based on the above encoding/encryption strategy, the propagation through this layer is formalized in Algorithm 5. This algorithm is similar to Algorithm 1, except for that it iterates through filter groups (each containing up to r filters) instead of individual filters; this way, we can gain a speed-up up to a factor of r . Interestingly, the output ciphertexts, when used as input for next layer, become cross-channel packed, which can thus be processed as described in the previous subsection.

Algorithm 5: Propagation Through Convolutional Layer l with Cross-Filter Packing

```

1 for  $k' \in \{0, \dots, \lceil \frac{\epsilon_l}{r} \rceil - 1\}$  do
2    $\triangleright$  iterating each filter group;
3   for  $(u, v) \in \{0, \dots, \tilde{\gamma}_{l+1} - 1\}^2$  do
4      $\hat{C}_{k',u,v}^{(l+1)} \leftarrow 0$ ;  $\triangleright$  initialize each output;
5      $(u', v') \leftarrow (\delta_l \cdot u, \delta_l \cdot v)$ ;
6     for  $(x, y) \in \{0, \dots, \gamma_l - 1\}^2$  do
7       for  $i \in \{0, \dots, \alpha_l - 1\}$  do
8          $\hat{C}_{k',u,v}^{(l+1)} \oplus = \hat{C}_{i,u'+x,v'+y}^{(l)} \otimes \hat{F}_{i,x,y}^{(l,k')}$ ;
9       end
10    end
11     $\hat{C}_{k',u,v}^{(l+1)} \leftarrow \hat{C}_{k',u,v}^{(l+1)} \otimes \hat{C}_{k',u,v}^{(l+1)}$ ;  $\triangleright$  activation
12  end
13 end

```

VI. EVALUATION

We implement the LHE-based inference scheme and run it on a moderate platform, i.e., a computer with Intel 2.6 GHz CPU that runs Ubuntu 20.04, for performance evaluation.

A. CNN Models and LHE Parameters

We use the CNN models described in Section II-B with $c \in \{1, 2, 3, 4\}$ and $f \in \{1, 2\}$. In the following, we use *CNN c-f* (e.g., *CNN 2-1*) to denote a CNN model with c convolutional layers (CLs) and f fully-connected layers (FLs). All experiments use the MNIST dataset [32] to classify the ten handwritten digits and each input image of 28×28 .

We employ CKKS [21] of the SEAL library [33] as the LHE scheme. Different polynomial modulus N are used to match different CNN configurations. Each plaintext has $S = \frac{N}{2}$ slots encoding up to S values. We adopt $N = 8192$ and $N = 16384$ which support a maximal coefficient modulus bit length of 218 and 438, respectively, to attain a 128-bit security level [34]. Since each CL or FL (including square activation) requires two levels of homomorphic multiplication, we adjust the polynomial modulus and coefficient modulus to make the LHE scheme to support different settings of CNNs. The detailed parameters are listed in Table I.

Table I: The SEAL parameters for different CNN structures

CNN models	N	Coefficient Modulus	Levels
CNN 1-2	8192	{34,30,30,30,30,30,34}	6
CNN 2-1	8192	{34,30,30,30,30,30,34}	6
CNN 2-2	16384	{40,30,30,30,30,30,30,40}	7
CNN 3-1	16384	{40,30,30,30,30,30,30,30,40}	8
CNN 3-2	16384	{40,30,30,30,30,30,30,30,30,40}	9
CNN 4-1	16384	{40,30,30,30,30,30,30,30,30,30,40}	10
CNN 4-2	16384	{40,30,30,30,30,30,30,30,30,30,30,40}	11

B. Evaluation Results

1) *Computation Time of LHE Operations:* We first measure the computation time of \oplus , \otimes , *Rot* and *CMul* with $N = 16384$ and various encryption levels. The results (averaged over 5000 measurements) are presented in Table II. As we can see, \otimes has the highest cost, followed by *Rot* whose cost is around 80% of \otimes , followed by *CMul* whose cost is about 15-20% of \otimes , and \oplus has the lowest cost. With the level increases, the costs for \otimes , *Rot* and *CMul* all increase linearly.

Table II: Execution time (μs) of LHE operations ($N = 16384$)

Level	\oplus	\otimes	<i>Rot</i>	<i>CMul</i>
2	93	6434	4542	1645
3	127	10106	7311	2467
4	172	14466	10719	3273
5	209	19757	14995	4137
6	253	25931	20057	5018
7	298	33139	25916	5935
8	345	39953	31722	6741
9	397	49835	40167	7942
10	443	57791	47144	8731
11	498	68374	56366	9895

2) *Scalability with Varying n (number of simultaneously-available inputs):* We experiment with CNN 3-2 model to evaluate the impact of $n \in \{16, 32, 64, 128, 256, 512\}$. The cross-channel or the cross-filter optimizations are applied whenever possible and the packing parameter r is computed according to the afore-described design.

Table III presents the computation time for encoding/encrypting initial input data and model parameters (in the columns labelled *Inputs*, *Filters* and *Weights*), and propagating through the layers (in the columns labelled *CL1-3*, *FL1-2*, and *Square* for activation function). The table also shows the total time for each forward propagation round (in the column labelled *Total*) and the averaged time for each input image (in the column labelled *Amortized*). As we can see, the total time increases with n while the amortized time (i.e., the average time for processing each input image) decreases. This demonstrates the following trade-off: the smaller is the scale of simultaneously-available input, the shorter is the delay for obtaining the inference result (indicated by column *Total*) and the lower is the system throughput (indicated by column *Amortized*). Meanwhile, the difference in amortized time is not significant when compared to the difference in the input size. Specifically, as n changes from 16 to 512, the amortized time changes only from 2.855s to 1.145s. This indicates that, our proposed design has good *scalability* in terms of that *its performance increases with the size of simultaneously-*

available inputs and meanwhile the performance does not degrade significantly when the input size is small.

3) *Comparison with CryptoNets and E2DM:* We compare the performance of our scheme with CryptoNets and E2DM, which are also based on LHE and the most related to our scheme. As the LHE systems employed by the compared schemes are not CKKS, which is used in our scheme, and the reported evaluation results [23] for them are obtained at different platforms, we do not directly compare in terms of measured computation time. Instead, we choose to count the numbers of LHE operations that each of the schemes need to conduct when they are given the same input. Also note that, E2DM supports only one convolutional layer, so comparison is conducted based on the CNN 1-2 model. Both E2DM and our scheme takes 64 images as parallel inputs, while CryptoNets takes 4096 images as parallel inputs (as its best performance is attained when all the 4096 slots are used).

Table IV shows the main comparison results among the three schemes. Comparing CryptoNets with the other schemes, CryptoNets has the highest total cost due to the large input size; in fact, even when the number of simultaneously-available inputs is smaller, CryptoNets still needs such cost since it is not adaptive to input size. When the size of simultaneously-available inputs is 4096, it has the lowest amortized cost. Specifically, it needs only $7.3 \otimes$ operations for each input images, by average, while E2DM needs $7.3 \otimes$, 5.5 Rot and 5 CMul operations, and our scheme needs $9.1 \otimes$ and 6 Rot operations.

However, the above comparison does not indicate that E2DM is more efficient than our scheme, because it only counts the number of LHE operations but does not consider the impact of encryption level. Table V shows the distribution of the LHE operations at different levels. As we can see, the LHE operations of E2DM occur at higher levels than our scheme. Together with the level-specific LHE operation costs shown in Table II, E2DM should incur higher cost.

As we can also see from Table IV, both CryptoNets and our scheme demand the highest encryption level of 6, while the level needed by E2DM is 8; note that, as shown by Table II, higher level implies most costly LHE operations. Regarding input encryption, E2DM and our scheme use the same packing method when the input size is 64 and thus have the same cost; CryptoNets has higher cost due to large input size. Regarding model encryption and preprocessing, our scheme has higher cost in encryption than E2DM, but E2DM needs to preprocess weight matrices which is not needed by our scheme; nevertheless, these are just one-time cost.

Overall, the comparisons indicate that, *our scheme is more efficient than E2DM mainly due to the smaller encryption level that we need.* Also, *CryptoNets has the lowest amortized cost but this is attainable only when a large number of inputs are simultaneously available.*

4) *Applicability to Different CNN Models:* To show the applicability of our model to generic CNN models, we evaluate our scheme with the CNN models whose configurations and

Table III: Computation Time for CNN 3-2 (unit: second)

(n, r)	Inputs	Filters	Weights	CL1	Square	CL2	Square	CL3	Square	FL1	FL2	Total	Amortized
(16,32)	8.076	2.967	4.668	22.535	2.013	15.008	0.916	0.920	0.018	3.560	0.704	45.674	2.855
(32,16)	8.108	2.974	4.683	21.829	1.943	13.780	0.886	0.927	0.018	3.236	0.692	43.311	1.353
(64,8)	8.464	6.188	7.297	44.310	4.022	24.790	0.912	1.740	0.032	3.835	0.713	80.354	1.256
(128,4)	8.409	12.347	12.170	88.434	8.074	47.035	0.880	3.261	0.058	5.110	0.690	153.542	1.2
(256,2)	8.769	25.088	22.355	177.42	16.026	91.092	0.911	6.676	0.118	8.65	0.707	301.598	1.178
(512,1)	8.742	48.978	41.712	344.842	32.435	179.136	0.885	12.971	0.224	15.145	0.696	586.334	1.145

Table IV: Numbers of LHE operations at every stages of CNN 1-2. Input size: 4096 for CryptoNets; 64 for E2DM and our scheme. Each single value in inputs and parameters encryption represent the number of encryption times and each value in Square row represents the number of ciphertext-ciphertext multiplication operations. **The tuples represent the number of LHE operations in the order of \oplus , \otimes , Rot and $CMul$. The 2-tuples, 3-tuples and 4-tuples match the first 2, 3 and 4 operations respectively.**

	Our Scheme	E2DM	CryptoNets
LHE Level	6	8	6
Enc. Inputs	49	49	784
Enc. Filter	196	196	196
Enc. Weight1	256	4	16384
Enc. Weight2	64	1	640
Preprocess Weight1		(1024,0,608,768)	
Preprocess Weight2		(138,0,44,148)	
CL1	(192,196,0)	(192,196,0)	(12288,12544)
Square	4	4	256
FL1	(576,256,384)	(512,256,320,256)	(16320,16384)
Square	64	1	64
FL2	(63,64,0)	(77,10,29,64)	(630,640)
Total	(831,584,384)	(781,467,349,320)	(29238,29888)
Amortized	(13.9,1.6)	(12.2,7.3,5.5,5)	(7.1,7.3)

Table V: Number of LHE operations at different levels.

	Our Scheme				E2DM			
Level	\oplus	\otimes	Rot	$CMul$	\oplus	\otimes	Rot	$CMul$
7	-	-	-	-	192	196	-	-
6	-	-	-	-	-	4	-	-
5	192	196	-	-	256	-	320	256
4	-	4	-	-	256	256	-	-
3	576	256	384	-	-	1	-	-
2	-	64	-	-	64	-	26	64
1	63	64	-	-	13	10	3	-

parameters listed in section VI-A. Due to space limit, we show only the results of two settings in Tables VI and VII.

As in Table VI, when our scheme is applied to CNN 2-1 with 16 parallel inputs, to compute inference from the inputs takes 17.271 seconds, which is 1.079 seconds for each input. With the setting, our scheme performs $87.1 \otimes$ and 6 Rot operations for each of its 16 input. CryptoNets performs $30.1 \otimes$ for each of its 4096 inputs; however, if it has only 16 inputs available, it performs 7705.6 \otimes operations per input, which is around 82 times higher. Similar trends can be observed from Table VII, except that the amortized cost increases as the scale of the model increases, which is reasonable. Hence, *our scheme has good applicability and scalability with varying size of simultaneously-available inputs under various CNN models.*

VII. RELATED WORKS

We briefly discuss the related works as follows.

Table VI: LHE operations and time for CNN 2-1 (Our scheme: n=16, r=16).

	LHE Operations		Time
	Our Scheme	CryptoNets	Our Scheme
Enc. Inputs	225	784	3.183
Enc. Filters	149	2384	2.12
Enc. Weights	40	640	0.561
Total	189	3024	2.681
CL1	(1200,1225)	(92928,94864)	15.882
Square	25	1936	0.251
CL2	(112,100,16)	(25536,25600)	0.859
Square	4	64	0.021
FL1	(110,40,80)	(630,640)	0.258
Total	(1422,1394,96)	(119094,123104)	17.271
Amortized	(88.9,87.1,6)	(29.1,30.1)	1.079

Table VII: LHE operations and time for CNN 4-2 (Our Scheme: n=128, r=16).

	LHE operations		Time
	Our Scheme	CryptoNets	Our Scheme
Enc. Inputs	441	784	20.036
Filters	133	2128	6.150
Weights	320	1184	14.471
Total	453	3312	20.621
CL1	(1944,2025,0)	(55296,57600)	133.093
Square	81	2304	4.579
CL2	(2352,1764,784)	(57200,57600)	112.451
Square	196	400	7.368
CL3	(315,324,0)	(8960,9216)	11.85
Square	9	256	0.222
CL4	(48,36,16)	(2288,2304)	1.128
Square	4	16	0.059
FL1	(576,256,384)	(960,1024)	5.452
FL2	(63,64,0)	(150,160)	0.822
Total	(5298,4759,1184)	(124854,130880)	277.024
Amortized	(41.4,37.2,9.3)	(15.2,16)	2.164

A. LHE-based Schemes

Schemes based on LHE were proposed in [22]–[27], [30]. Among them, CryptoNets [22] is one of the first works applying the packing technique [20] for inference based on a CNN model. Assuming the simultaneous-availability of a large number of inputs, it packs one value from each input into a ciphertext and thus process the inputs in parallel to attain a high level of amortized efficiency. E2DM [23] packs a matrix into a ciphertext and proposes an efficient algorithm to multiply two encrypted matrices; it also proposes packing and efficient processing for CNN models with one convolutional layer, but does not handle more general CNN models. PROUD [27] applies the techniques and introduces parallel execution to further speed up the system. We also

apply LHE to our proposed framework, but focus to design the inference scheme applicable for more generic CNN models and scalable to the availability of parallel inputs.

B. MPC-based Schemes

Several recent works [1]–[8], [26], [27], [35], [36] propose two-party computations schemes that require interactions between the client and server while the computation is being performed, which could cause high communication overheads and latency. Among them, for example, MiniONN [3] and GAZELLE [4] split the inputs so that both client and server hold additive secret shares of input, and garbled circuits are employed for non-linear computation. DELPHI [5] extends GAZELLE and designs a hybrid scheme that generates neural network architecture configurations to balance the trade-offs between performance and accuracy. Three-party computation-based schemes are also proposed in [9], [10], [12], [13] and four-party computation-based schemes are explored in [13]–[15]. However, these three-party and four-party computation-based schemes all introduced under the assumption of a honesty-majority.

C. TEE-based Schemes

Schemes [16], [17], [37] were also proposed based on TEE. Among them, Citadel [16] preserves data and model privacy in distributed training by partitioning code to two parts, i.e., data handling code executed by multiple training enclaves and model handling code executed by an aggregation enclave. CHEX-MIX [17] combines HE with TEE to protect data and model confidentiality as well as verify the computation integrity, when the client and server are mutually distrustful. The inference process are completely executed inside enclave with inputs encrypted with HE and attested model parameters. We also adopt TEE in our proposed framework. However different from the related works, we minimize the involvement of TEE only for essential works such as LHE key management and decryption/re-encryption of final results; we assign the most workload to the REE of server which has more resources than the TEE.

VIII. CONCLUSIONS

In this paper, we propose a new framework based on symbiotic integration of LHE and TEE, which enables collaboration among mutually-untrusted three parties. We also propose a generic and efficient LHE-based inference scheme, along with optimizations, as an important performance-determining component of the framework. We have implemented the proposed system on a moderate platform, and conducted extensive evaluations to show that, our proposed system is applicable and scalable to various settings, and it has better or comparable performance when compared with the state-of-the-art solutions which are more restrictive in applicability and scalability.

REFERENCES

- [1] P. Mohassel and Y. Zhang, "Secureml: A system for scalable privacy-preserving machine learning," in *2017 IEEE symposium on security and privacy (SP)*. IEEE, 2017, pp. 19–38.
- [2] B. D. Rouhani, M. S. Riazi, and F. Koushanfar, "Deepsecure: Scalable provably-secure deep learning," in *Proceedings of the 55th annual design automation conference*, 2018, pp. 1–6.
- [3] J. Liu, M. Juuti, Y. Lu, and N. Asokan, "Oblivious neural network predictions via minion transformations," in *Proceedings of the 2017 ACM SIGSAC conference on computer and communications security*, 2017, pp. 619–631.
- [4] C. Juvekar, V. Vaikuntanathan, and A. Chandrakasan, "{GAZELLE}: A low latency framework for secure neural network inference," in *27th USENIX Security Symposium (USENIX Security 18)*, 2018, pp. 1651–1669.
- [5] P. Mishra, R. Lehmkuhl, A. Srinivasan, W. Zheng, and R. A. Popa, "Delphi: A cryptographic inference service for neural networks," in *29th USENIX Security Symposium (USENIX Security 20)*, 2020, pp. 2505–2522.
- [6] N. Chandran, D. Gupta, A. Rastogi, R. Sharma, and S. Tripathi, "Ezpc: Programmable and efficient secure two-party computation for machine learning," in *2019 IEEE European Symposium on Security and Privacy (EuroS&P)*. IEEE, 2019, pp. 496–511.
- [7] M. S. Riazi, M. Samragh, H. Chen, K. Laine, K. Lauter, and F. Koushanfar, "{XONN}:{XNOR-based} oblivious deep neural network inference," in *28th USENIX Security Symposium (USENIX Security 19)*, 2019, pp. 1501–1518.
- [8] M. S. Riazi, C. Weinert, O. Tkachenko, E. M. Songhori, T. Schneider, and F. Koushanfar, "Chameleon: A hybrid secure computation framework for machine learning applications," in *Proceedings of the 2018 on Asia conference on computer and communications security*, 2018, pp. 707–721.
- [9] P. Mohassel and P. Rindal, "Aby3: A mixed protocol framework for machine learning," in *Proceedings of the 2018 ACM SIGSAC conference on computer and communications security*, 2018, pp. 35–52.
- [10] S. Wagh, S. Tople, F. Benhamouda, E. Kushilevitz, P. Mittal, and T. Rabin, "Falcon: Honest-majority maliciously secure framework for private deep learning," *arXiv preprint arXiv:2004.02229*, 2020.
- [11] M. Baryalai, J. Jang-Jaccard, and D. Liu, "Towards privacy-preserving classification in neural networks," in *2016 14th annual conference on privacy, security and trust (PST)*. IEEE, 2016, pp. 392–399.
- [12] A. Patra and A. Suresh, "Blaze: blazing fast privacy-preserving machine learning," *arXiv preprint arXiv:2005.09042*, 2020.
- [13] N. Koti, M. Pancholi, A. Patra, and A. Suresh, "{SWIFT}: Super-fast and robust {Privacy-Preserving} machine learning," in *30th USENIX Security Symposium (USENIX Security 21)*, 2021, pp. 2651–2668.
- [14] H. Chaudhari, R. Rachuri, and A. Suresh, "Trident: Efficient 4pc framework for privacy preserving machine learning," *arXiv preprint arXiv:1912.02631*, 2019.
- [15] M. Byali, H. Chaudhari, A. Patra, and A. Suresh, "Flash: fast and robust framework for privacy-preserving machine learning," *Cryptology ePrint Archive*, 2019.
- [16] C. Zhang, J. Xia, B. Yang, H. Puyang, W. Wang, R. Chen, I. E. Akkus, P. Aditya, and F. Yan, "Citadel: Protecting data privacy and model confidentiality for collaborative learning," in *Proceedings of the ACM Symposium on Cloud Computing*, 2021, pp. 546–561.
- [17] D. Natarajan, W. Dai, and R. Dreslinski, "Chex-mix: Combining homomorphic encryption with trusted execution environments for two-party oblivious inference in the cloud," *Cryptology ePrint Archive*, 2021.
- [18] "Intel xeon scalable processor reference for lenovo thinksystem servers," <https://lenovopress.lenovo.com/lp1262-intel-xeon-sp-processor-reference#term=SGX>, 2021.
- [19] Z. Brakerski and V. Vaikuntanathan, "Efficient fully homomorphic encryption from (standard) lwe," *SIAM Journal on computing*, vol. 43, no. 2, pp. 831–871, 2014.
- [20] N. P. Smart and F. Vercauteren, "Fully homomorphic simd operations," *Designs, codes and cryptography*, vol. 71, no. 1, pp. 57–81, 2014.
- [21] J. H. Cheon, A. Kim, M. Kim, and Y. Song, "Homomorphic encryption for arithmetic of approximate numbers," in *International Conference on the Theory and Application of Cryptology and Information Security*. Springer, 2017, pp. 409–437.
- [22] R. Gilad-Bachrach, N. Dowlin, K. Laine, K. Lauter, M. Naehrig, and J. Wernsing, "Cryptonets: Applying neural networks to encrypted data with high throughput and accuracy," in *International conference on machine learning*. PMLR, 2016, pp. 201–210.
- [23] X. Jiang, M. Kim, K. Lauter, and Y. Song, "Secure outsourced matrix computation and application to neural networks," in *Proceedings of*

the 2018 ACM SIGSAC Conference on Computer and Communications Security, 2018, pp. 1209–1222.

- [24] F. Bourse, M. Minelli, M. Minihold, and P. Paillier, “Fast homomorphic evaluation of deep discretized neural networks,” in *Annual International Cryptology Conference*. Springer, 2018, pp. 483–512.
- [25] R. Dathathri, O. Saarikivi, H. Chen, K. Laine, K. Lauter, S. Maleki, M. Musuvathi, and T. Mytkowicz, “Chet: an optimizing compiler for fully-homomorphic neural-network inferencing,” in *Proceedings of the 40th ACM SIGPLAN Conference on Programming Language Design and Implementation*, 2019, pp. 142–156.
- [26] P. Xie, B. Wu, and G. Sun, “Bayhenn: combining bayesian deep learning and homomorphic encryption for secure dnn inference,” *arXiv preprint arXiv:1906.00639*, 2019.
- [27] S. Xie, B. Liu, and Y. Hong, “Privacy-preserving cloud-based dnn inference,” in *ICASSP 2021-2021 IEEE International Conference on Acoustics, Speech and Signal Processing (ICASSP)*. IEEE, 2021, pp. 2675–2679.
- [28] F. McKeen, I. Alexandrovich, A. Berenzon, C. V. Rozas, H. Shafi, V. Shanbhogue, and U. R. Savagaonkar, “Innovative instructions and software model for isolated execution.” *Hasp@ isca*, vol. 10, no. 1, 2013.
- [29] W.-j. Lu and J. Sakuma, “Crypt-cnn (ii): Cryptographically evaluate non-linear convolutional neural network,” *CSS 2017*, pp. 773–780, 2017.
- [30] E. Chou, J. Beal, D. Levy, S. Yeung, A. Haque, and L. Fei-Fei, “Faster cryptonets: Leveraging sparsity for real-world encrypted inference,” *arXiv preprint arXiv:1811.09953*, 2018.
- [31] W.-j. Lu, Z. Huang, C. Hong, Y. Ma, and H. Qu, “Pegasus: Bridging polynomial and non-polynomial evaluations in homomorphic encryption,” in *2021 IEEE Symposium on Security and Privacy (SP)*. IEEE, 2021, pp. 1057–1073.
- [32] Y. LeCun, “The mnist database of handwritten digits,” <http://yann.lecun.com/exdb/mnist/>, 1998.
- [33] “Microsoft SEAL (release 3.7),” <https://github.com/Microsoft/SEAL>, Sep. 2021, microsoft Research, Redmond, WA.
- [34] K. Laine, “Simple encrypted arithmetic library 2.3.1,” *Microsoft Research* <https://www.microsoft.com/en-us/research/uploads/prod/2017/11/sealmanual-2-3-1.pdf>, 2017.
- [35] W.-j. Lu and J. Sakuma, “Crypt-cnn (i): Secure two-party computation of large-scale matrix-vector multiplication,” 2017.
- [36] Z. Huang, W.-j. Lu, C. Hong, and J. Ding, “Cheetah: Lean and fast secure two-party deep neural network inference,” *Cryptology ePrint Archive*, 2022.
- [37] F. Tramer and D. Boneh, “Slalom: Fast, verifiable and private execution of neural networks in trusted hardware,” *arXiv preprint arXiv:1806.03287*, 2018.